Ozean Journal of Applied Sciences 2(4), 2009
ISSN 1943-2429

Hydrocarbon Reservoir Mapping and Volumetric Analysis Using Seismic and Borehole Data over "Extreme" Field, Southwestern Niger Delta.

Adeoye, T. O. and *Enikanselu, P.A.

Department of Applied Geophysics, Federal University of Technology, P.M.B. 704, Akure. Nigeria.

*E-mail address for correspondence: pa.enikan@yahoo.com

Abstract *: Hydrocarbon reservoirs have been delineated and their boundaries mapped using direct indicators from 3-D seismic as well as borehole data over 'Extreme' Field, offshore Niger Delta. The research methodology involved horizon and fault interptretation to produce subsurface structural maps. Amplitudes of reflections were mapped to define the lateral boundary of the reservoir. The reservoir area extent was determined using the square grid template method. Wireline log signatures were employed to identify hydrocarbon bearing sands and compute reservoir petrophysical parameters for hydrocarbon pore volume determination.*

Well to seismic tie revealed that these reservoirs tied direct hydrocarbon indicators – bright and dim spots - on the seismic sections. The structure maps revealed fault assisted closures at the center of the field, which correspond to the crest of rollover anticlines and possibly served as the trapping medium.

Three hydrocarbon bearing reservoirs - R_1, R_2 and R_3 - were delineated. The reservoir porosity estimates varied from 0.22 to 0.31, hydrocarbon saturation 0.6 to 0.9 and thickness from 1.75 to 26.97 metres. The reservoir area extent deduced from the amplitude anomaly map varied from 9.79 to 11.88 km^2

Estimation of the volume of hydrocarbon in place revealed that R_1 has the least hydrocarbon accumulation of 60,708.67 cubic feet of gas while R_2 contained 43,407.70 barrels of oil and 123,019.78 cubic feet of gas in place. Reservoir R_3 contained an estimate of 110,323.09 barrels of oil and 321664.36 cubic feet of gas.

The study has shown the feasibility of integrating surface seismic and direct hydrocarbon indicators in mapping reservoir boundaries. Their integration with borehole data facilitated the evaluation of hydrocarbon pore volume.

INTRODUCTION

The knowledge of reservoir dimension is an important factor in quantifying producible hydrocarbon (Schlumberger, 1989). Among the needed information includes the thickness and area extent of the reservoir. These parameters are important because they serve as veritable inputs for reservoir volumetric analysis i.e. the volume of hydrocarbon in place (Edward, 1988). It is therefore imperative that they are determined with reasonable precision. Precise determination of reservoir thickness is best obtained on well logs, especially using the gamma ray and resistivity logs (Asquith, 2004). Because almost all oil and gas produced today come from accumulations in the pore spaces of lithologies like sandstones, limestone or dolomites, the gamma ray log can come in handy to help in lithology identification i.e to differentiate between the reservoir rock (sand) and the embedding shale (Asquith, 2004). If core data is available, other lithologies like limestone or dolomites can be identified (Kathleen, 1996). The resistivity log on the other hand, can be used for determining the nature of intersticial fluid i.e differentiating between (saline) water and hydrocarbon in the pore spaces of the reservoir rocks. Since these logs are recorded against depth, the hydrocarbon-bearing interval can be determined. Accurate mapping of the lateral dimension of the reservoir on the other hand, can be obtained from well logs, where abundantly available, or direct hydrocarbon indicartors (Brown et al, 1984). To use well logs to map the lateral dimension of the reservoir, the gas-oil and oil- water contacts are located on structure maps, (Cofeen, 1984). This process can be seriously hampered when, as is usually the case, limited borehole information from wells is available.

In this study, we have employed direct hydrocarbon indicators - bright spots, dim spots, flat spots and phase changes - on seismic sections in mapping reservoir area extent. These indicators are valuable mapping tools because they suggest the presence of hydrocarbons directly on seismic sections (Brown, 2004).

The Bright spot is a high amplitude reflection caused by the acoustic impedance contrast between the reservoir and the embedding medium (shale). In the hydrocarbon-bearing reservoir (e.g. gas sand), there is a lowering of the acoustic impedance due to hydrocarbon saturation compared to the embedding medium with high impedance. The dim spot is a decrease in amplitude of reflections over a short distance. The reflections appear 'dim' on the seismic sections. They are produced as a result of the contrast between the acoustic impedance of water sand, the embedding medium (shale) and that of the reservoir. The Flat spot is a horizontal reflection that is reflected from fluid to fluid interphases (fluid contact). Examples include gas–oil, gas-water, or oil-water contacts. The flat spot is easily identified by its flatness and unconformability with adjacent reflections (Brown, 2004). Phase change is the same as local waveshape change (Kathleen, 1996). Reflections switch character.across a fluid contact. This is as a result of significant change in acoustic properties between the gas sand above the hydrocarbon-water contact and the water sand beneath it (Brown, 2004).

Also, in mapping reservoir boundaries, studies of geologic structures that can hold hydrocarbon in place must be considered. Hydrocarbons are found in geologic traps, that is, any combination of rock structure that will keep oil and gas from migrating either vertically or laterally (Wan Qin, 1995). These traps can either be structural, stratigraphic or a combination of both. Structural traps can serve to prevent both vertical and lateral migration of the connate fluid (Cofeen, 1984). Examples of these include anticlines and flanks of salt domes. Stratigraphic traps include sand channels, pinchouts, unconformities and other truncations (Folami et al, 2008). According to Doust and Omatsola (1976), majority of the traps in the Niger delta are structural and to locate them, horizons are picked and faults mapped on seismic inlines and crosslines to produce the time structure map. This can reveal the structures that can serve as traps for the hydrocarbon accumulations. It is then possible to deduce the relevant petrophysical parameters from well logs, for the computation of the volume of hydrocarbon in place.

Location and Geology of the Study Area

The Niger delta forms one of the world's major hydrocarbon provinces and it is situated on the Gulf of Guinea on the west coast of central Africa (Southern Nigeria). It covers an area within longitudes 4ºE – 9ºE and latitudes 4ºN - 9ºN (Figure 1). It is composed of an overall regressive clastic sequence, which reaches a maximum thickness of about 12 km (Evamy et al, 1978).

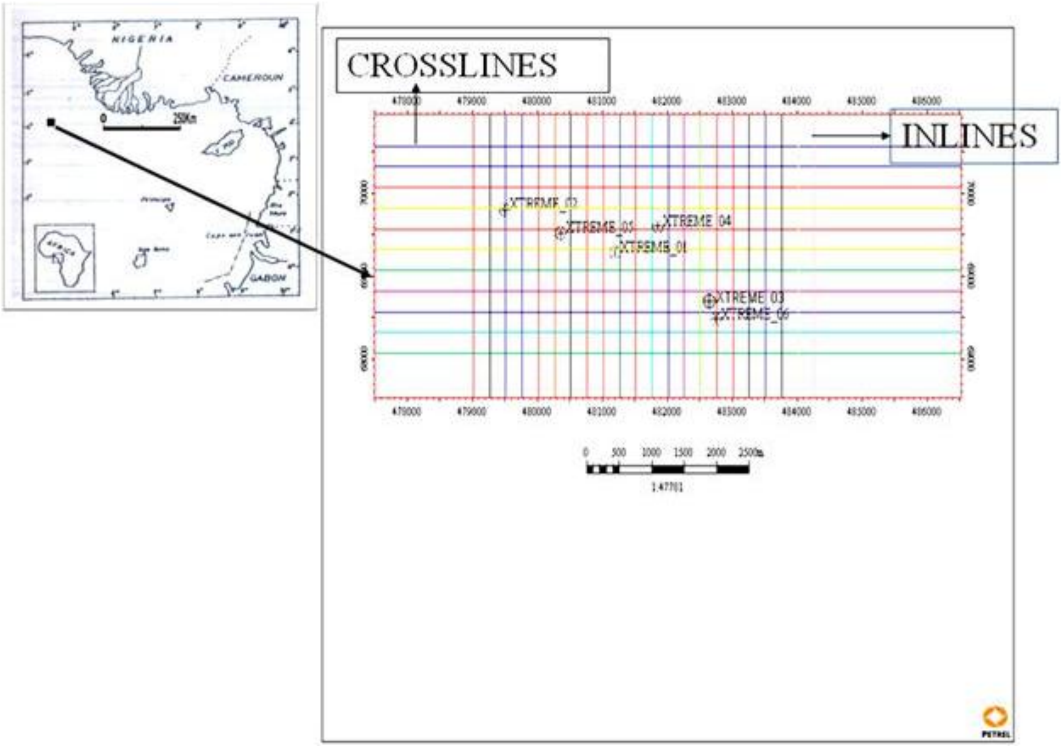

Fig 1: Location and Base Maps of the Study Area showing Seismic Lines and Well Logs

Lithostratigraphy

The Niger delta consists of three broad Formations (Short and Stauble, 1967): the continental top facies (Benin Formation), the Agbada Formation and the Akata Formation. The Benin Formation is the shallowest of the sequence and consists predominantly of fresh water-bearing continental sands and gravels. The Agbada Formation underlies the Benin Formation and consists primarily of sand and shale and is of fluviomarine origin. It is the main hydrocarbon-bearing window. The Akata Formation is composed of shales, clays and silts at the base of the known delta sequence. They contain a few streaks of sand, possibly of turbiditic origin. The thickness of this sequence is not known for certain, but may reach 7000m in the central part of the delta (Short and Stauble 1967).

Reservoir Rocks

Petroleum in the Niger Delta is produced from sandstone and unconsolidated sands predominantly in the Agbada Formation. The characteristics of the reservoirs in the Agbada Formation are controlled by depositional environment and the depth of burial. Known reservoir rocks are Eocene to Pliocene in age and are often stacked, ranging in thickness from less than 15 meters with about 10% having greater than 45 meters thickness (Evamy *et al*., 1978). The thicker reservoirs represent composite bodies of stacked channels (Doust and Omatsola, 1990). Based on reservoir geometry and quality, Kulke (1995) described the most important reservoir types as point bars of distributary channels and coastal barrier bars intermittently cut by sand-filled channels. Doust and Omatsola (1990) described the primary Niger delta reservoirs as Miocene paralic sandstones with 40% porosity, 2 Darcys permeability, and a thickness of 100 meters. The lateral variation in reservoir thickness is strongly controlled by growth faults; the reservoir thickening towards the fault within the down-thrown block (Weber and Daukoru, 1975). The grain size of the reservoir sandstone is highly variable with fluvial sandstones tending to be coarser than their delta front counterparts. Point bars fine upward, and barrier bars tend to have the best grain sorting. Much of this sandstone is nearly unconsolidated, some with a minor component of argillo-silicic cement (Kulke, 1995). Porosity slowly decreases with depth because of the age of the sediments.

Traps and Seals

Most known traps in Niger delta fields are structural although stratigraphic traps are not uncommon. The structural traps developed during synsedimentary deformation of the Agbada paralic sequence (Evamy et al, 1978; Stacher, 1995). Structural complexity increases from the north (earlier formed depobelts) to the south in response to increasing instability of the under-compacted, over-pressured shale. Doust and Omatsola (1990) described a variety of structural trapping elements, including those associated with simple rollover structures clay-filled channels, structures with multiple growth faults, structures with antithetic faults and collapsed crest structures. On the flanks of the delta, stratigraphic traps are likely as important as structural traps. In this region, pockets of sandstone occur between diapiric structures. Towards the delta toe (base of distal slope) this alternating sandstone-shale sequence gradually grades to essentially sandstone.

The primary seal rock in the Niger delta is the interbedded shale within the Agbada Formation. The shale provides three types of seals — clay smears along faults, interbedded sealing units against which reservoir sands are juxtaposed due to faulting and vertical seals (Doust and Omatsola, 1990). On the flanks of the delta, major erosional events of early to middle Miocene formed canyons that are now clay-filled. These clays form the top seal for some important offshore field locations.

MATERIALS AND METHODS

The data used in the study include digital suites of well logs, checkshot data, inlines and crosslines of 3-D seismic sections and base map of the study area; all of which were imported into the interactive '*Petrel*' workstation. The checkshot data was used for the well-to-seismic tie of the hydrocarbon reservoirs and displayed on the seismic lines they intersected. Horizons were tracked on these reflections, on both inlines and crosslines across the field to produce the time structure (isochron) maps. Also, the depth structure maps were produced from this, using velocity information derived from checkshot data. .

The relevant wireline log signatures were employed to identify hydrocarbon-bearing reservoirs and computing reservoir petrophysical parameters like porosity, water saturation, net reservoir thickness, gross reservoir thickness and the ratio of net to gross thickness. In addition, fluid contacts were delineated. These logs include: gamma ray log (lithology identification), volume of shale log (porosity correction), density and neutron log (delineating fluid contacts), resistivity and water saturation logs (identifying pore fluid type).

According to Brown (2004), mapping the lateral boundary of the reservoir can be done (with the interactive workstation) by extracting and mapping amplitudes of direct hydrocarbon indicators like bright spots on the seismic sections. In this study, amplitudes of the horizons were extracted and presented in map form to produce reflection amplitude map. This was used to define the reservoir boundary. The surface area extent covered by the reservoir was estimated from this using the grid template method.

The volume of hydrocarbon-in-place (hydrocarbon pore volume, HCPV) was calculated using Aly (1989):

$$HCPV = V\Phi\, N/G(1 - S_W)$$

where

V = Volume of hydrocarbon; which equals the product of reservoir area extent (A) and its thickness (t). The thickness of the reservoir was obtained by taking average values from well log (gamma ray, neutron and density logs) signatures.

Φ = Average effective porosity obtained from the density log.

S_W = Average water saturation values from water saturation log.

N/G = ratio of net-to-gross thickness of the reservoir as obtained from the gamma ray

logs.

DISCUSSION OF RESULTS

Prelimnary study on the well logsrevealed three hydrocarbon-bearing reservoirs - R_1, R_2 and R_3 - within depth interval of 8,000ft (2,440m) and 11,500ft (3,507m), Figures 2 and 3.

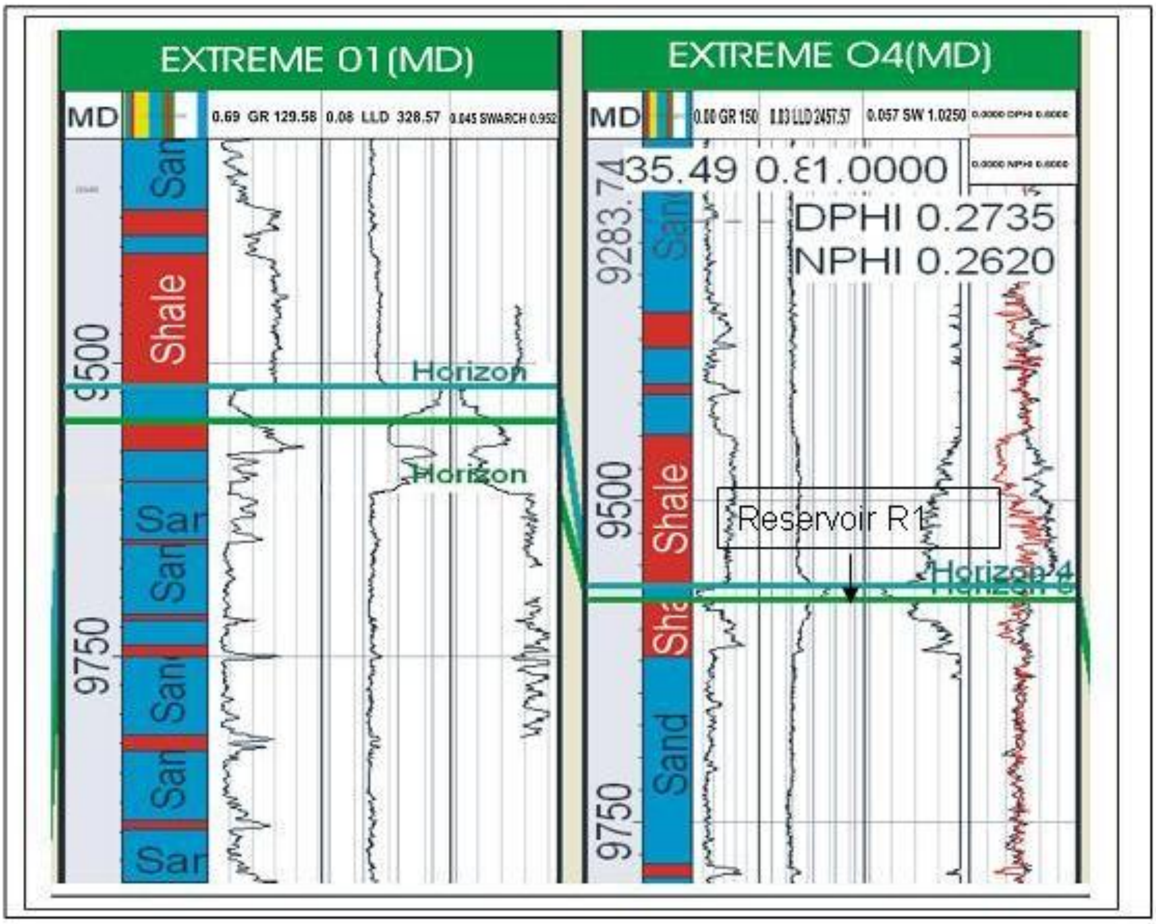

Figure 2: Reservoir R_1 delineated on the well logs.

The salient reservoir petrophysical parameters obtained from these reservoirs are shown in Tables 1, 2 and 3. It could be observed that hydrocarbon saturation and effective porosity estimates in reservoir R_1 varied from 0.62 to 0.85 and 0.24 to 0.31 respectively. The net thickness of the reservoir varied from 5.77ft (1.76m) to 71.24ft (21.73m). In reservoir R_2, effective porosity varied between 0.26 and 0.24 while hydrocarbon saturation varied between 0.60 and 0.69. The net thickness of the reservoir varied between 20.56ft (6.27m) and 55.5ft (16.92m). For reservoir R_3, effective porosity varied between 0.22 and 0.27 while hydrocarbon saturation varied between 0.65 and 0.93. The net thickness of the reservoir varied between 41.4ft (12.63m) and 88.4ft (26.96m).

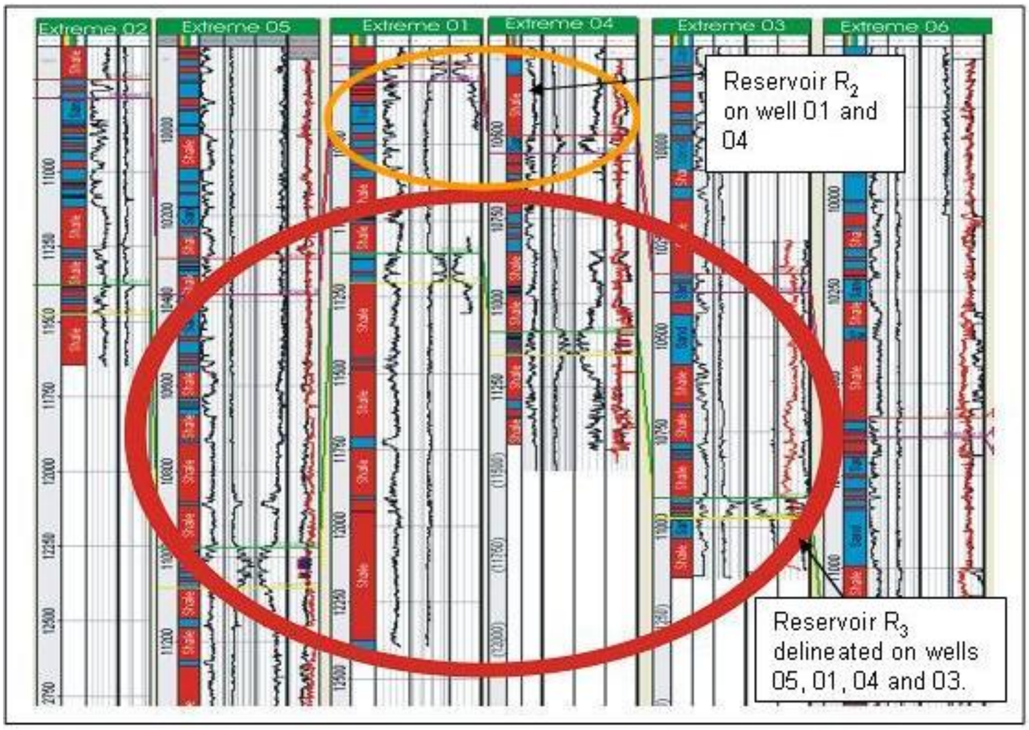

Figure 3: Well sections showing Reservoirs R_2 and R_3 delineated on well Logs.

Table 1: Computed petrophysical Parameters from Reservoir $R_{1.}$

Well	Top (Md) ft (m)	Bottom (Md) ft (m)	Thickness (Gross) ft (m)	Thickness (Net) ft (m)	Net/Gross	Porosity (Effective)	Hydrocarbon Saturation
04	9,566 (2,917)	9,577 (2,920)	25 (7.63)	25 (7.63)	0.56	0.31	0.85
01	9,517 (2,902)	9,600 (2,928)	25 (7.63)	25 (7.63)	0.75	0.24	0.62

Table 2: Computed Petrophysical Parameters from Reservoir $R_{2.}$

Well	Top(Md) ft [m]	Bottom(Md) ft [m]	Thickness(Gross) ft [m]	Thickness(Net) ft [m]	Net/Gross	Effective Porosity	Hydrocarbon Saturation
04	10,550 (3,217)	10,594 (3,231)	44.00 (13.42)	20.56 (6.27)	0.39	0.26	0.60
01	10,541 (3,215)	10,590 (3,229)	70.10 (21.38)	55.50(16.93)	0.78	0.24	0.69

Table 3: Computed petrophysical parameter from Reservoir R_3

Well	Top(Md) ft [m]	Bottom(Md) ft [m]	Thickness(Gross) ft [m]	Thickness(Net) ft [m]	Net/Gross	Effective Porosity	Hydrocarbon Saturation
04	11,125 (3,393)	11,197 (3,415).	72.23 (22.03)	41.4 (12.63)	0.57	0.22	0.93
01	11,151 (3,401)	11,249. (3,430)	98.40 (30.01)	74.10 (22.60)	0.75	0.25	0.85
03	10,898 (3,323)	11,021 (3,361)	123.83 (37.76)	88.4 (26.92)	0.71	0.25	0.65
05	11,022 (3,361)	11,117 (3,390)	95.82 (30.05)	54.3 (16.56)	0.56	0.27	0.90

Well-to-seismic tie revealed that the hydrocarbon bearing reservoirs are associated with direct hydrocarbon indicators on seismic sections. Figure 4 is an example from reservoir R_1. The top of reservoir R_1 tied a dim spot at the two way travel time of 2465ms i.e. depth of 9566ft (2917.63m). Similarly, Reservoir R_2 and R_3 tied bright spots on the seismic sections (not shown).

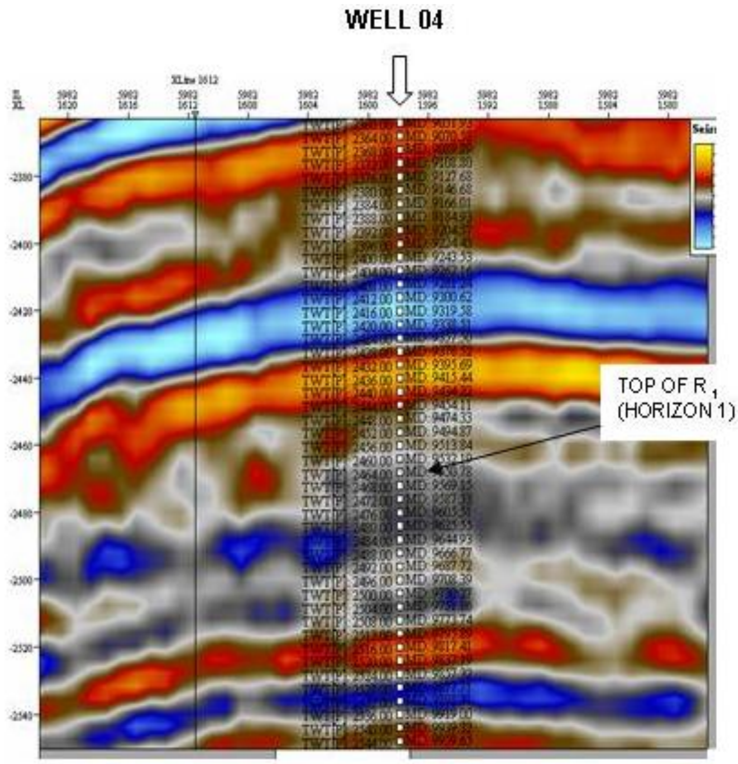

Figure 4: Well-to-seismic tie of reservoir R_1 from well 04 (showing dim spots).

Since the bright and dim spots are indicative of hydrocarbon presence, the lateral boundaries of these reservoirs were mapped from the amplitudes. In the research, horizon picking were initiated on the bright spot and dim spots reflections. Their amplitudes were extracted and presented in map form. Figure 5 is the amplitude map of horizon one. Reservoir R_1 is seen as an anomalous low amplitude zone on the map in the center of the field and correlated with the gas-bearing reservoir as revealed on neutron-density overlay, from well 4 in Figure 2. The total estimated area covered by the gas sand was 9.79 km^2. The same analysis was performed for reservoirs R_2 and $R_{3;}$ that is, reflection amplitude maps were generated for horizon two and three respectively and the zone of anomalous high amplitudes were used to map the boundaries of the reservoir (They matched bright spots on seismic sections). The reservoir area extent estimation from the square grid method revealed that reservoir R_2 covered an area of 10.56 km^2 while reservoir R_3 covered an area extent of 11.88 km^2.

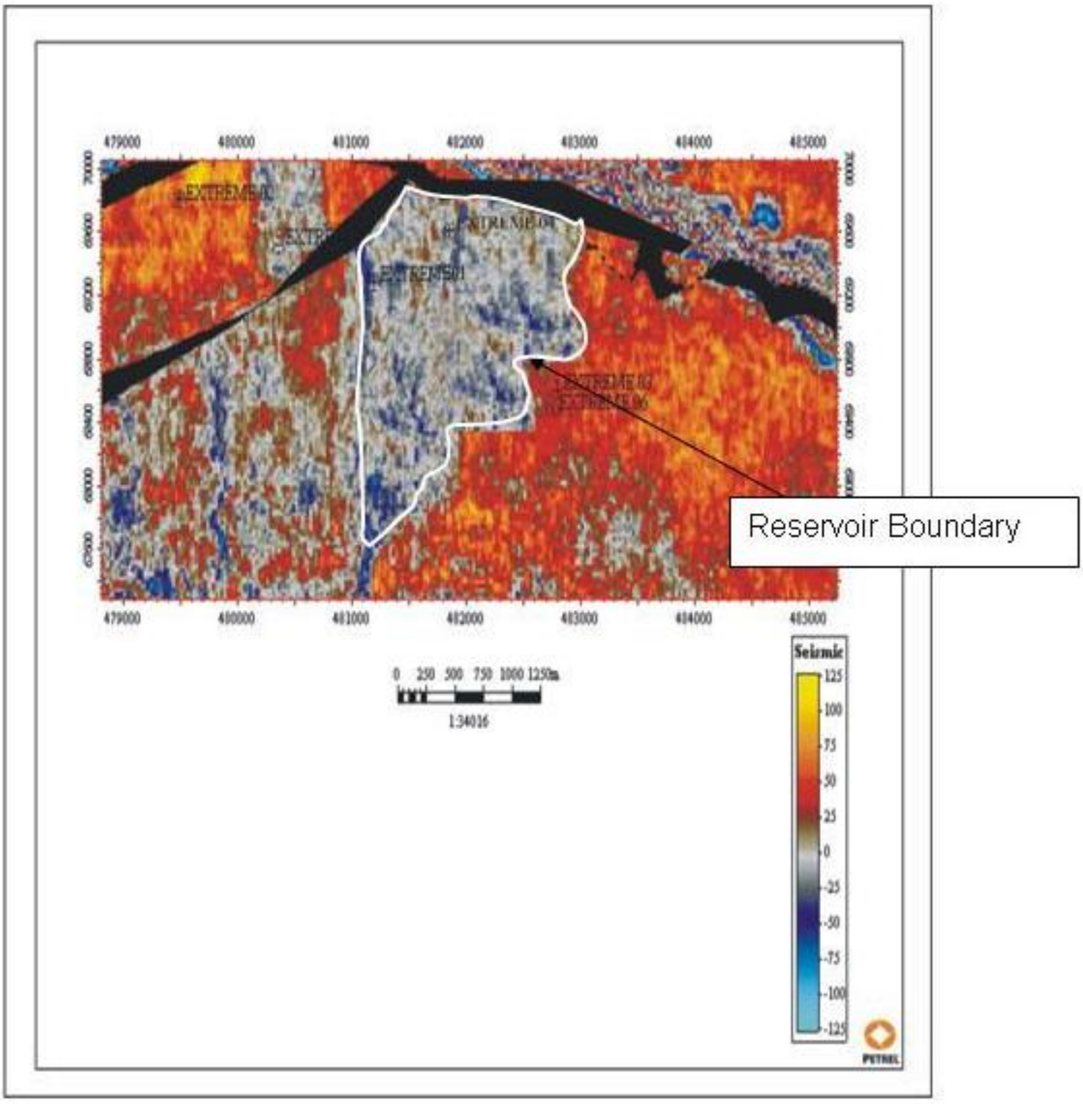

Figure 5: Reflection Amplitude Map of Horizon one delineating the Lateral boundary of Reservoir R_1.

Horizon and fault interpretation were carried out for subsurface structural interpretation. In all, three horizons (One, Two and Three) and five faults – F_1 through F_5 - were mapped on seismic sections over the entire field, (Figure 6).

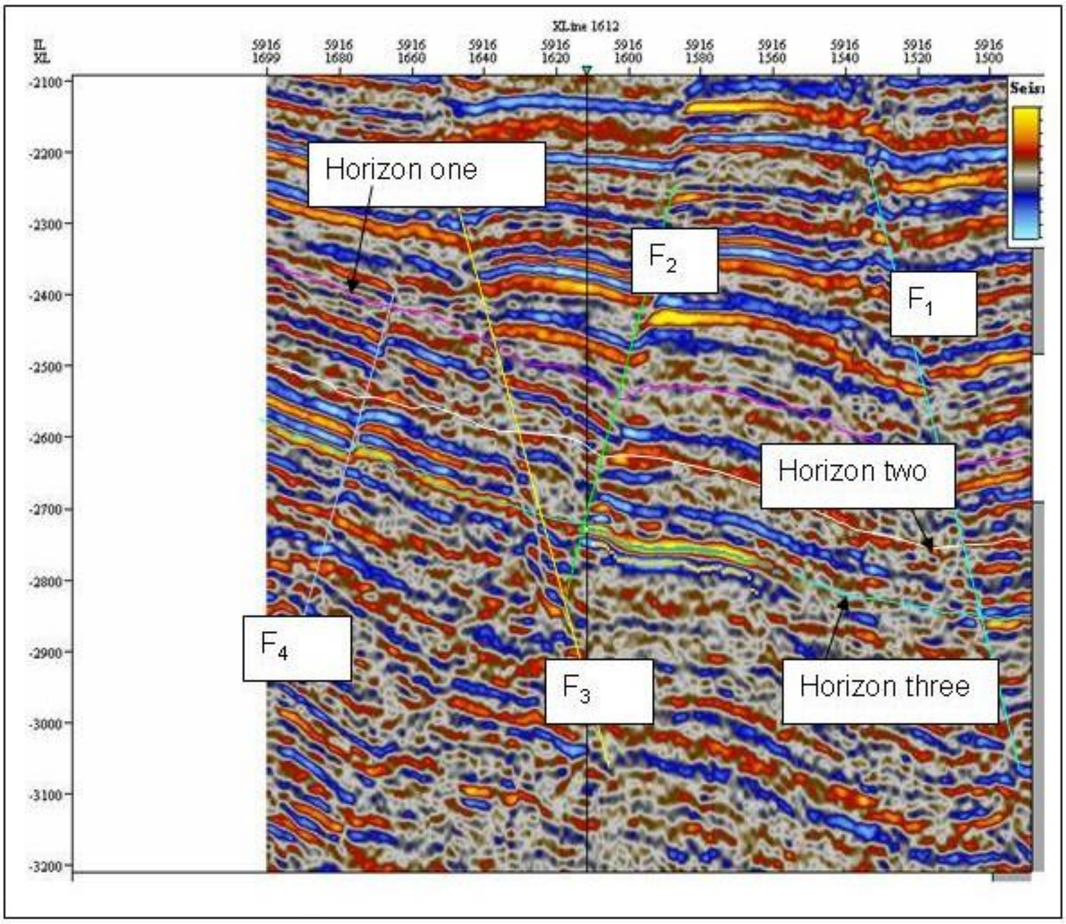

Figure 6: Typical seismic section (Inline 1699), showing Horizons and Faults.

Figures 7 and 8 are respectively the time and depth structure maps generated from 3-D structural interpretation. The principal structure responsible for hydrocarbon entrapment in the field is a structural high located at the center of the field which probably corresponded to the crest of the roll over structure observed on the seismic sections, Figure 6. This was observed as fault assisted closures on the time structure maps of each horizon. Figure 7 is the time structural map of horizon one. Structural highs are observed in the northeast and in the center of the field while structural lows are observed in the southwest. Using the information on this map, the crest of the roll over structure (structural high), antithetic fault F_2 and growth fault F_3 act as good traps for the hydrocarbon accumulations in reservoir R_1 at the center of the field. The other faults identified on the map include F_1 (a growth fault), F_4 and F_5 (minor faults), and fault F_2, which is an antithetic fault.

The depth structure map generated revealed that for horizon one, the depth to the top of hydrocarbon ranges between 9,500ft (2,897.5m) and 9,566ft (2,917.63m), Figure 8. Similarly, for horizon two (not shown), the depth to the top of hydrocarbon ranged between 10,500ft (3,202.5m) and 10,700ft (3,233m) at the center of the field while for horizon three, depth to the top of hydrocarbon at the center of the field varies between 11,000ft (3,355m) and 11,200ft (3,401m).

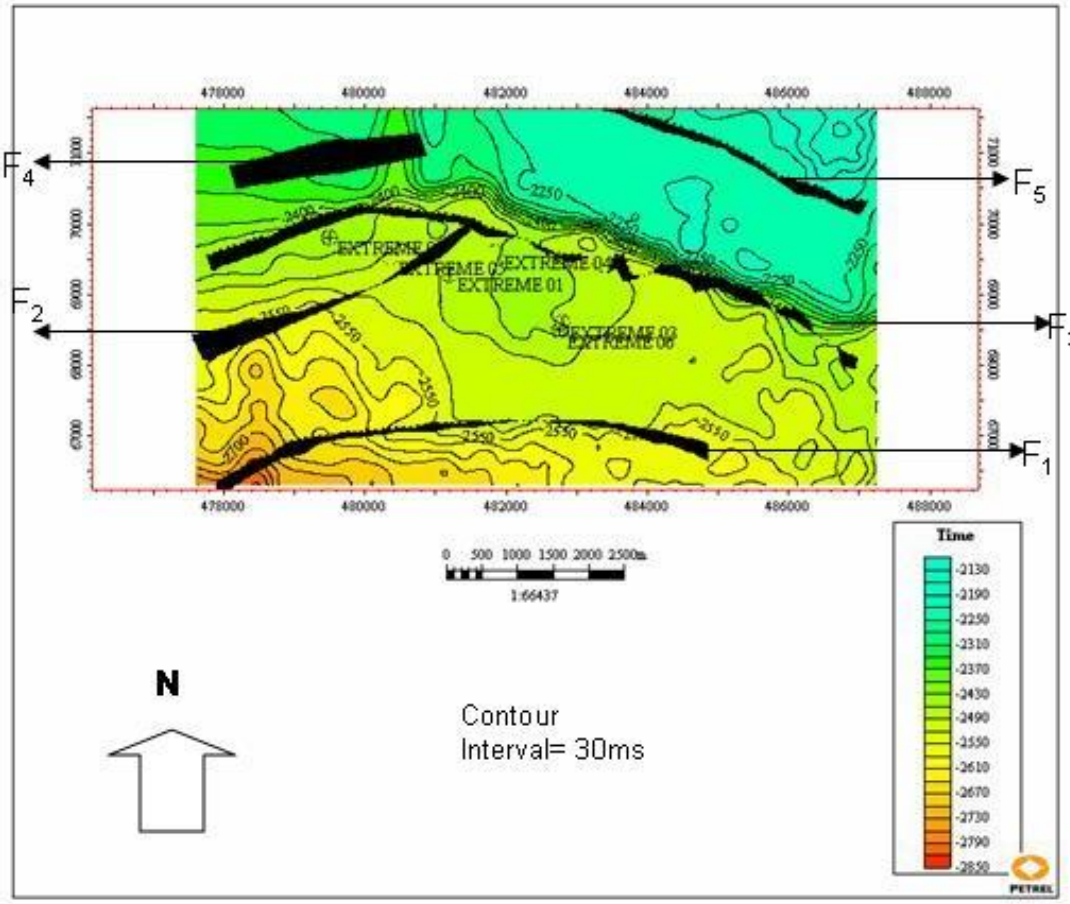

Figure 7: Time structural map of Horizon one.

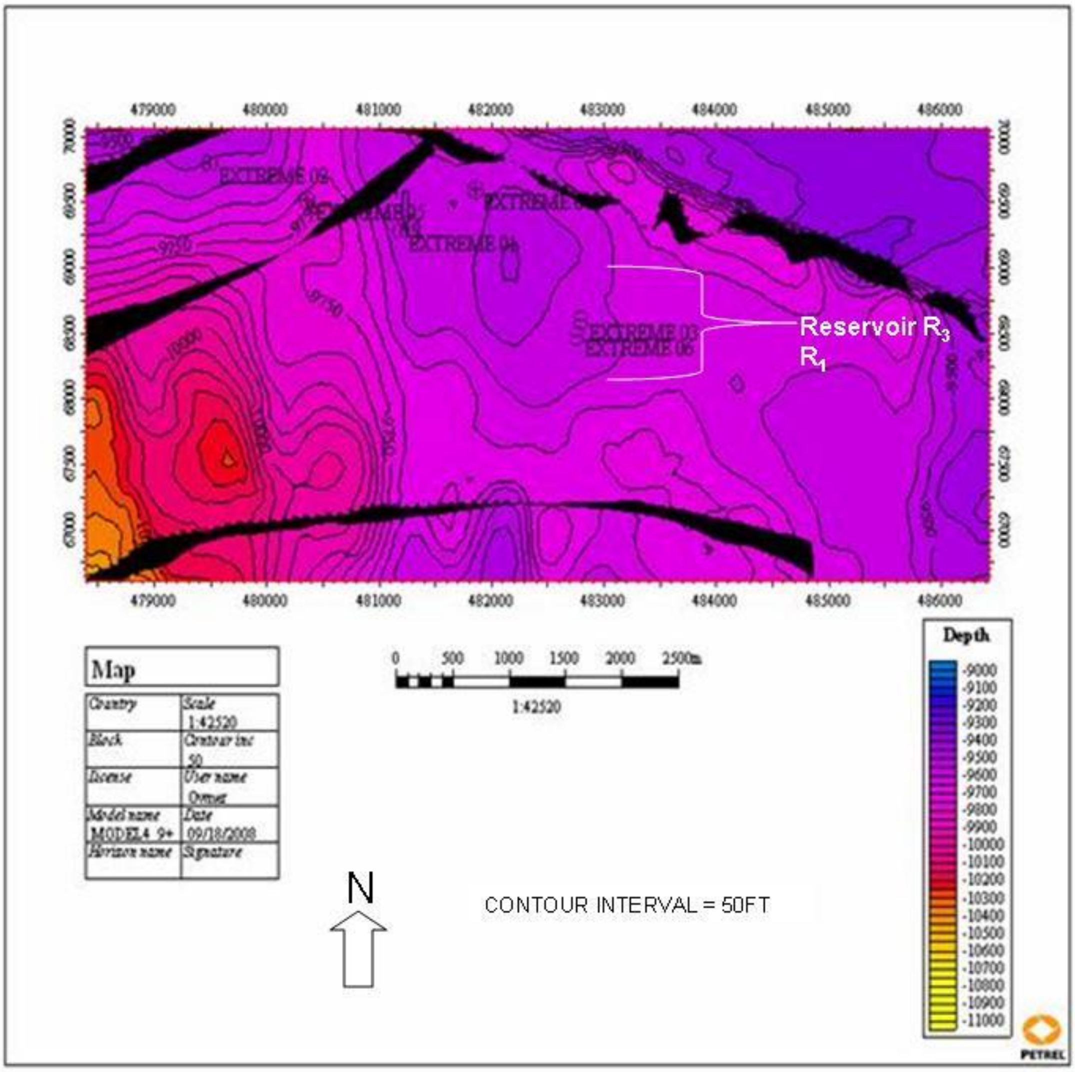

Figure 8: Depth Structure Map of Horizon One

Hydrocarbon pore volume estimates showed that Reservoir R_1 has a volume of 60708.67 cubic feet of gas, Reservoir R_2 has oil in place of 43,407.70 barrels and gas in place of about 123,019.78 cubic feet while Reservoir R_3 has the highest hydrocarbon accumulation with a total estimate of 110,323.09 barrrels of oil and 321,664.36 cubic feet of gas. The detailed analysis is shown in Tables 3 and 4.

Table 3: Results of Oil Volume Estimates in Reservoirs R_1 and R_2.

Reservoir	Porosity	Hydrocarbon Saturation	Thickness (Oil) [ft] m	Net/Gross	Area [m^2]	Hydrocarbon [Oil] in Place [Barrels]
R_2	0.25	0.65	15.00 (4.57)	0.88	10560	43,407.700
R_3	0.26	0.80	30.00 (9.10)	0.78	11880	110,323.09

Table 4: Results of Gas Volume Estimates in Reservoirs R_1, R_2 and R_3.

Reservoir	Porosity	Hydrocarbon Saturation	Reservoir Thickness ft [m]	Net/Gross	Area (km^2) or ft^2	Gas In Place (Cubic-ft)
R_1	0.26	0.80	52.90(16.13)	0.75	(9.79) 32120.99	60,708.67
R_2	0.25	0.65	23.00(7.02)	0.95	(10.56)34647.36	123,019.78
R_3	0.28	0.27	25.00(7.63)	1.00	(11.88)38978.28	321,664.36

CONCLUSION

In this study, we have embarked on the delineation and mapping of hydrocarbon- bearing reservoirs from surface seismic sections and well logs within the depth interval of 8,000ft (2,440m) and 11,500ft (3,507m). in this process, we have carried out 3-D structural interpretation and estimation of the volume of hydrocarbon-in-place in the reservoirs.

From well log analysis, three hydrocarbon-producing reservoirs (R_1, R_2 and R_3) were identified. Well-to-seismic tie revealed that hydrocarbon bearing reservoirs were associated with direct hydrocarbon indicators (Bright spots and dim spots) on the seismic sections. Three horizons were studied and five faults mapped for the purpose of carrying out 3-D subsurface structural interpretation. This was used in generating the time structure maps. From the maps, it was observed that the principal structure responsible for hydrocarbon entrapment in the field was the anticlinal structure at the center of the field which tied to the crest of the rollover structure seen on the seismic sections.

Direct hydrocarbon indicators were used to map the reservoir boundary. They were seen on the reflection amplitude maps as high amplitude zones (bright spots) and low amplitude zones (dim spots). Reservoir area extent obtained from square grids revealed that reservoir R_1 had an area estimate of 9.79 km^2; reservoir R_2 10.56 km^2 while reservoir R_3 covered about 11.88 km^2.

Estimation of the volume of hydrocarbon in place revealed that reservoir R_1 had the least hydrocarbon estimate of 60,708.67 cubic feet of gas while reservoir R_2 contained 43,407.70 barrels and about 123,019.78 cubic feet of gas in place. Reservoir R_3 contained an estimate of 110,323.09 barrels of oil and 321,664.36 cubic feet of gas.

ACKNOWLEDGEMENT

The authors are grateful to the department of Applied Geophysics, Federal University of Technology, Akure, Nigeria for permitting us the use of the data for the research. Also, Miss Omolola Aluko, of the Secretariat of the Academic Staff Union of Universities in the institution, helped in transforming our scrawl into a typescript.

REFERENCES

Aly, S. A. (1989). Evaluation of petrophysical properties of reservoir rocks using well logging analysis in Abu Ghyaradig Basin, Western Egypt", Unpublished Ph.D.thesis, Faculty of science, Kain Shams University, Cairo, Egypt.

Asquith G, (2004). Basic Well Log Analysis. American Association of Petroleum Geologists, Methods in exploration series: American Association of Petroleum Geologists, Tulsa, Oklahoma, No 16. pp. 12-135

Brown A. R. (2004). Interpretation of three-dimensional seismic data: American Association of Petroleum Geologists, Memoir 42 SEG investigations in geophysics, No 9, pp. 12 -89

Brown A.R, Wright, R.M (1984). Mapping of producible gas sand in the northsea, Geophysics, vol. 49, pp. 686-714

Coffen, J. A. (1984). Interpreting seismic data: Penwell Publishing Company, Tulsa Oklahoma. pp. 39-118.

Doust, H., and Omatsola, E., (1990). Niger Delta, in, Edwards, J. D., and Santogrossi, P.A., eds., Divergent/passive Margin Basins, AAPG Memoir 48: Tulsa, American Association of Petroleum Geologists, pp. 239-248.

Evamy, B.D., Haremboure, J., Kamerling, P., Molloy, F.A., and Rowlands, P.H., (1978). Hydrocarbon habitat of Tertiary Niger Delta: American Association of Petroleum Geologists Bulletin, v. 62, pp. 1-39.

Folami T.O, Ayuk M.A and Adesida A. (2008). Identification of Hydrocarbon reservoirs using Seismic Attributes and Geocellular Modelling: A case Study from “Tyke” Field, Niger Delta: Nigeria Association of Petroleum Geologists Bulletin 2008. pp. 30-32.

Kulke, H., (1995), Nigeria, in, Kulke, H., ed., Regional Petroleum Geology of the World. Part

II: Africa, America, Australia and Antarctica: Berlin, Gebrüder Borntraeger, pp.143-172.

Schlumberger (1989). Log Interpreation, Principles And Application: Schlumberger Wireline And Testing, Houston,Texas, pp. 21-89

Short S. and Stauble G. (1967). Outline of Geology of Niger Delta: American Association of Petroleum Geologists Bullettin pp. 761-768

Stacher, P., (1995). Present understanding of the Niger Delta hydrocarbon habitat, in, Oti, M.N., and Postma, G., eds., Geology of Deltas: Rotterdam, A.A. Balkema, pp. 257-267.

Wan Qin (1995). Reservoir delineation using 3-D seismic data of the Ping Hu field, East China, Unpublished MSc thesis, university of Colorado Boulder p 6-8

Weber, K. J., and Daukoru, E.M., (1975). Petroleum geology of the Niger DeltaProceedings of the Ninth World Petroleum Congress, volume 2, Geology: London, Applied Science Publishers, Ltd., pp. 210-221.